Optical Modeling of the Entire Visual Field of the Eye

Published in J Opt Soc Am A Opt Image Sci Vis. 2023 Jul 1;40(7):D7-D13. https://doi.org/10.1364/JOSAA.488033 .

This is the author's accepted manuscript (AM) and not the published version.

MICHAEL J. SIMPSON

Simpson Optics LLC, 3004 Waterway Ct, Arlington, TX 76012, USA
Corresponding author mjs1@outlook.com

Received XX Month XXXX; revised XX Month, XXXX; accepted XX Month XXXX; posted XX Month XXXX (Doc. ID XXXXX); published XX Month XXXX

Vision is rarely evaluated scientifically at very large visual angles, despite being used continuously in everyday life. Furthermore, raytrace calculations indicate that peripheral optical properties are different for a pseudophakic eye, and even though this is rarely noted by patients, it is probably the cause of bothersome "negative dysphotopsia". Simplified paraxial parameters that characterize the basic properties of phakic and pseudophakic eyes are collected together here as a baseline, and then raytracing is used to show that input angles of about 60°, which correspond to obstruction by the nose, eyebrow and cheek, illuminate a retinal hemisphere. At larger angles in the temporal direction, the image with an IOL reaches a limit due to vignetting at about a 90° input angle to the optical axis, in comparison to 105° with the Gullstrand-Emsley eye model, and 109° for the most realistic gradient index crystalline lens model. Scaling the far peripheral vision region more accurately may lead to benefits relating to intraocular lenses (IOLs), diseases of the peripheral retina, widefield fundus images and myopia prevention.

1. INTRODUCTION

The fundamental optical properties of the eye are often described using paraxial parameters, which is consistent with foveal vision being by far the most important visual region[1]. As visual angle increases, paraxial properties are generally assumed to be still valid for a considerable range of angles, but without any clear evaluation of what the accuracy might be. At very large visual angles, there have been evaluations that are related to imaging the photoreceptors in the periphery[2,3], but there is rarely any discussion or evaluation of the very limit of the visual field, and what a person sees there. This is consistent with perimetry being the main clinical measurement method, with a standard perimeter only measuring to 90° in the temporal direction, rather than to the visual limit, which is often assumed to be 105° [4]. Equipment that can make measurements at larger angles is not readily available.

Recent evaluations of bothersome "dark shadows" that are seen by some intraocular lens (IOL) patients in the far periphery[5,6] have led to questions about far peripheral vision. The use of IOLs has increased in recent decades, and an evaluation of one county in Minnesota found that about 7 % of the entire population had at least one IOL, mostly in an older age group, with about 50% of those aged over 75 having at least one IOL [7]. This is consistent with surgical cases exceeding 3.5 million per year in the US. Recent theoretical calculations indicate that all eyes with an IOL (often called pseudophakic eyes) probably have a difference in vision in the far periphery compared to their own earlier phakic eye, whether or not they see bothersome shadows[5,6], though IOL patients rarely report changes.

A second modern concern is the increase of myopia, with a prediction that half the population of the world will be myopic by 2050[8]. The far periphery has never been considered to be a potential contributing factor, but there are still no clear methods that will prevent or reverse myopia. Clinical research into this topic has looked into at least two specific visual angles, foveal vision for near work at small visual angles[9], and the mid-periphery[10], but concepts that appeared to work in animals have been found to have a limited effect in humans[11]. Subjects in clinical studies presumably also used their entire visual field, however, and if there was an unexpected confounding signal for eye growth from a different part of the visual field it may have gone undetected, particularly because focusing on near objects, and the defocus characteristics of the mid-periphery, had compelling rationales as the cause of myopia. The origins of the eye go back to where detecting peripheral predators was more important than reading, and monitoring the entire visual field may yield new insight into potential treatments for myopia[4]. This would be for young eyes as the eye is growing, rather than older eyes with IOLs. However, IOL patients have been specifically describing problems with their vision in the far periphery now for nearly 25 years (negative dysphotopsia)[12], with little recognition of this in the broader vision community, and there is likely to be overlap between these two topics for any new methods that evaluate this visual region.

Recent research relating to large visual angles has also led back to paraxial parameters like the "focal length", the "nodal point, the "equivalent focal length (efl)", and the "effective focal length (efl)" (with the last two being the same thing)[13–15]. Simple parameters for the eye may generally be known, but they are rarely summarized together, or compared to similar properties of the pseudophakic eye. These paraxial characteristics are described here, along with calculations that characterize the limiting visual angle.

2. BACKGROUND

Fig. 1. depicts some important parameters for the eye that are primarily related to optical power. Fig. 1(a) has the Gullstrand-Emsley Eye model[1], where the internal lens has a single refractive index, rather than the gradient index that is a distinctive feature of the crystalline lens. Despite this, the principal planes and nodal planes are in similar locations to those for more complex eye models. Only collimated light is considered here, in order to simplify the discussions, with the cornea simplified to a single surface, because the power of the entire cornea has its optical effect just anterior to the cornea.

The principal planes are where an "equivalent lens" that had the same paraxial optical properties as the eye would be placed, with air on the front, and fluid on the back. In 1905, Conrad Beck gave a clear explanation for why two principal planes are needed, using an analogy that is no longer used[16]: "It is impossible to find any single lens that, placed in any one position, will act in a similar way to a compound lens; if, however, we take a thin single lens of the correct focal length, and place it at P to receive the rays of light, and then rapidly shift it to P' to discharge these rays, it will act in an exactly similar manner to the original lens. Such a lens can be found for all optical systems that have a focus." This description captures the essence of the optical effect. For the optical system of the eye the two principal planes are very close together, and for many purposes they can be considered to be superimposed. With collimated light, only the 2nd principal plane is used anyway, and this is just inside the eye at about 2 mm from the anterior corneal vertex.

The distance from the 2nd principal plane to the focus is the "focal length" of the eye, and this is illustrated in a different manner in Fig. 1(b) using a reduced eye[17]. The entire power of the eye acts at the front surface, and this is the physical location of the principal plane, with air to the left and fluid to the right. This has optical properties that are equivalent to the original eye, with the cornea of this model acting as the equivalent thin lens. In order to have the correct focal length the corneal radius is 5.56 mm and the axial length is 22.22 mm

The "nodal points" are often defined using a ray at an angle[18], but the 2nd nodal point in Fig. 1(a) is actually easily found by dividing the focal length by the refractive index of the image medium[15]. This is often called the EFL, which is a term that has a long history as the "equivalent focal length" for a compound lens system, but which has more recently been thought to mean "effective focal length". These terms are equivalent, and the latter is now in widespread use, though EFL is used more as a symbol for the distance than as an acronym for the words.

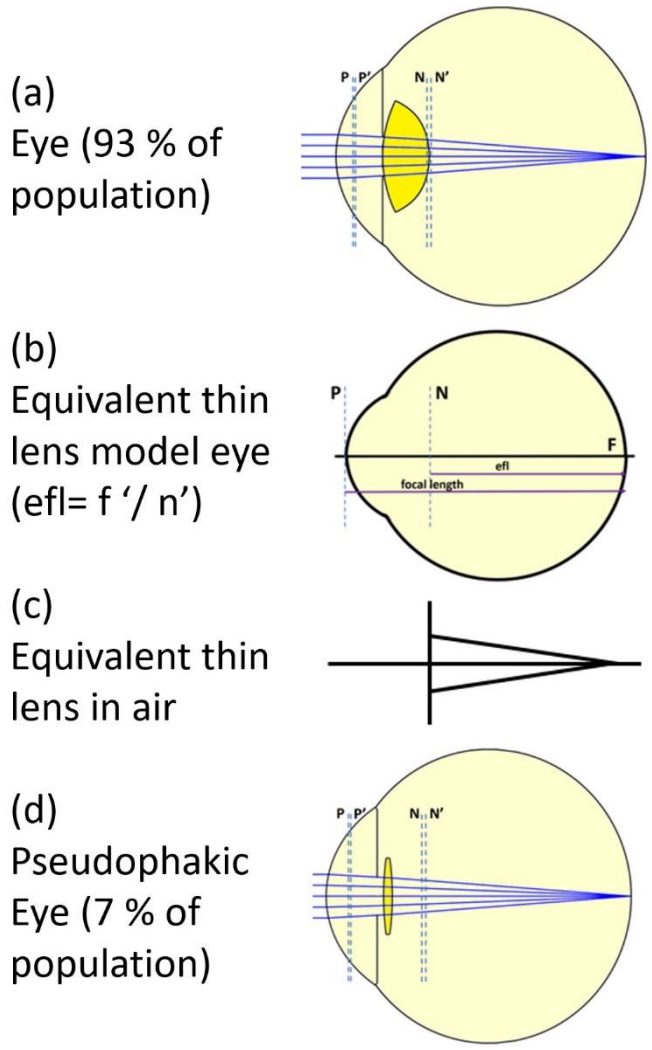

Fig. 1. Equivalent optical systems for collimated light. (a) Gullstrand-Emsley schematic eye. (b) Reduced eye, where the cornea acts as the equivalent thin lens for the entire eye (with a different corneal radius and axial length). (c) A different equivalent thin lens that is located in air at the nodal point also has the same paraxial optical properties (the fluid is removed). (d) In the pseudophakic eye, the crystalline lens has been replaced by a thin plastic lens. The iris also moves to the posterior, and it is typically no longer in contact with the internal lens.

One aspect of the nodal point is that a thin lens in air could be placed there that would have the same paraxial optical properties as the original eye, though this would be a different equivalent lens to the one that could be placed at the principal point. This is depicted schematically in Fig. 1(c), and Figs. 1(a-c) collectively illustrate some general parameters of the phakic eye.

The pseudophakic eye in Fig. 1(d) has the same physical dimensions as the phakic eye in Fig. 1(a), and although the intraocular lens is much thinner and smaller, it has a broadly similar power to the original phakic lens, and the principal and nodal points of the eye are in similar locations. The iris moves to the posterior following cataract surgery, and although in the phakic eye the iris is normally in contact with the crystalline lens, in the pseudophakic eye there is typically a gap between the iris and the IOL. An average value of 0.5 mm was found in an evaluation of OCT images, but with a

range from 0 to 1 mm, and a strong axial length trend, where shorter eyes have smaller gaps[19]

In practice, although the powers of the individual lens surfaces, and the eye, are all important, it is difficult to use an error in power on its own to improve the refraction of the eye. In Fig. 1 all the examples are in focus for collimated light, but the powers would remain the same if the image plane moved, though the image would then be defocused. Additional information about where the image is focused is always needed, and detailed information about all the optical surfaces are actually needed in order to make an adjustment because the surfaces are widely separated.

When the object is not on the optical axis, rays traced at an angle through the nodal point can be used to find the image location on the retina. This is often assumed to extend beyond the paraxial regime, but it is only relatively recently that the distinction between paraxial rays and chief rays has been explored for this topic[13,20–22]. Imaging in the mid-periphery of the phakic eye has been evaluated recently in great detail without using paraxial assumptions because of interest in preventing myopia[23]. The original thinking behind this was that if the image is formed in front of the retina, then the eye would shorten to put it more in focus, for which there appeared to be a great deal of supporting evidence. This may now be thought of as a consequence rather than a cause of myopia[10], but the entire visual field is normally in use, and tracking as much of the retina as possible may ultimately lead to a solution.

Vision in the far periphery is of particular interest for IOL patients because of reports about bothersome dark shadows in the far periphery since about the year 2000[12]. There is still no complete consensus in the clinical community about the cause of this "negative dysphotopsia", and even the visual angles at which the shadows are seen is not typically measured. Perimetry is the main clinical test for the periphery, but standard equipment only reaches to 90°, and its main purpose is for other types of clinical measurement, rather than to evaluate visual phenomena. There is a need for a new simple method to specifically measure these types of detail. Perimetry measurements have actually found many shadowlike phenomena across the entire visual field in pseudophakes (including even the optic disc), but their locations have not generally been compared to the "bothersome" dark shadows that the subjects were reporting separately and the results are difficult to interpret[24,25]. The most solid data for the bothersome dark shadow locations is that a military salute will obscure them[6], which would normally correspond to a very large visual angle.

Optical modeling of the pseudophakic eye very clearly demonstrates, however, that it is simply not possible for light to pass through the optical portion of a conventional IOL and reach the far periphery because the light is vignetted at the IOL edge[6,26]. IOLs had never specifically been designed to provide vision over the complete range of visual angles, and even when negative dysphotopsia became a concern it seemed likely initially that the issue might be something to do with the corneal incision, or the lens itself, or capsular opacification, or some other unknown variable, rather than to be something related to the size of the IOL and to the far periphery[5,27].

Modeling the limiting region of the visual field is difficult for both phakic and pseudophakic eyes. The gradient index lens of the phakic eye has a complicated internal structure, and the outer lens surface also needs to have the correct shape. IOLs also have various shapes near their edge regions, and these are rarely described clearly by the manufacturers[28]. The lens haptics also have varying characteristics, and these can have an effect on peripheral rays, depending on their orientation[29]. The far periphery is also a region where there is low retinal resolution, very large aberrations, and perhaps also significant defocus. This paper evaluates both phakic and pseudophakic eye models, and it explores the limit of vision.

3. METHOD

The Zemax OpticStudio Professional raytrace software v22.2.1 (www.ansys.com) was used to model both phakic and pseudophakic eyes. Two different types of phakic eye were modeled, the Gullstrand-Emsley eye that has a lens with a constant refractive index, and a model eye that has been described previously[6,30,31] (Akram) that has a complex gradient index lens that is intended to represent a 70 year old eye[6] (an average age for cataract surgery). A single equibiconvex high refractive index IOL was used as a pseudophakic comparison, in an average model eye that has also been described before[5]. A spherical retina with a 12 mm radius was used for all the eyes. In each case, chief rays at a wavelength of 0.546 microns were traced through the center of the stop, and image locations where the chief rays intersected with the retina were determined. Angles were then calculated from 3 axial locations; the exit pupil, the 2nd nodal point, and the center of the retinal sphere.

For the eye model with the IOL, additional evaluations were performed. The light rays transmitted through the lens, light rays missing the lens, and the regions of the cornea intercepted by the rays, were all evaluated for different angles by rotating the eye around the corneal apex (in order to achieve improved control over the angles in Zemax). An 8 mm diameter clear aperture was placed at an arbitrary 10 mm in front of the corneal apex. This rotated with the input beam, and it was used as a reference to evaluate the portions of the input beam that were directed into the two main image regions. For the focused component, the 6 mm diameter IOL optic formed the limiting aperture. To evaluate light missing the IOL, a separate eye model was used where the anterior IOL optic surface was described using the multizone user-defined surface that is provided with Zemax. The central 6 mm diameter was made opaque using a central obscuration, the overall surface diameter was set to 20 mm, the IOL material was changed to fluid, and the posterior surface was set to a plano 20 mm diameter, to allow rays that missed the IOL to travel without obstruction to the retina. A Zemax macro was written to evaluate light energy for different angles using a square grid of input rays, with the evaluation including the energy losses due to Fresnel reflections at the optical surfaces. The rays were traced efficiently by using the "ray aiming" feature of Zemax to locate the limiting stop, a characteristic of the software that has also been used elsewhere to evaluate the apparent pupil location of the eye[32]. Details of the rays traced in Zemax were stored in a file for evaluation in Matlab. An energy adjustment for obscuration by the increasing ellipticity of the pupil was made by dividing values by 0.8 times the cosine of the retinal angle [26], and a vertical integration was made across radial point

spread functions, to give an approximation for retinal intensity that would be expected with even illumination from all visual angles.

4. RESULTS

The most realistic crystalline lens is depicted in Fig. 2, with rays input at 60° to the optical axis. The 3 axial points that are of particular interest are also identified, and lines are drawn from there to the intersection with the retina of the chief ray. The calculations in this paper do not include angle alpha, which on average is a rotation of 5° outwards in the horizontal direction from the optical axis to the visual axis, or any decentration of the pupil. This simplifies the discussion, and it is consistent with paraxial parameters. The 5 degrees is actually a beneficial extension of the highly linear angular relationship, adding 5 degrees beyond 0 in the negative direction, and it is included in papers that are more directly addressing clinical issues[5].

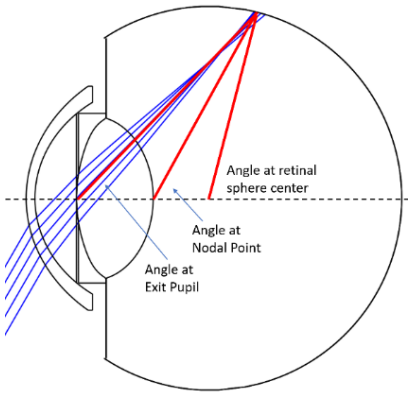

Fig 2. Akram model eye with a gradient index crystalline lens that has aspheric surfaces. Left eye from above. Light at an angle of 60° to the optical axis enters the eye, which has an iris with a 3mm pupil diameter. Lines are drawn to the chief ray intersection with the retina from the axial locations of the exit pupil, the 2nd nodal point, and the center of the retinal sphere.

The cross-sectional outer profiles of the 3 internal lenses are compared in Fig 3, with rays that enter the eye at 60° and pass through a 3mm diameter pupil. The Gullstrand-Emsley lens has spherical surfaces and no gradient index, and although it was never intended originally to be used at very large angles, it gives plausible results. The Akram 70 year old lens has aspheric outer surfaces that aim to simulate the contour of a real crystalline lens more accurately, along with a gradient index internal material. The IOL is much smaller than the crystalline lens.

Fig. 4. plots the internal angles from the 3 points of interest to the retinal intersections of the chief ray for the Akram model eye, along with just the angles relative to their own nodal point for the other two model eyes. Broadly similar relationships were found by Drasdo et al and Suheimat et al for different eye models[2,3]. The Akram model has the most complexity, and the model transmits rays up to 109° of input angle. The Gullstrand-Emsley model also transmits rays to 105°, but the IOL is much smaller, and the chief ray is vignetted at about 90°. It is also possible for light to miss the IOL completely and illuminate the retina directly, and it is highly likely that this is the fundamental cause of negative dysphotopsia[6].

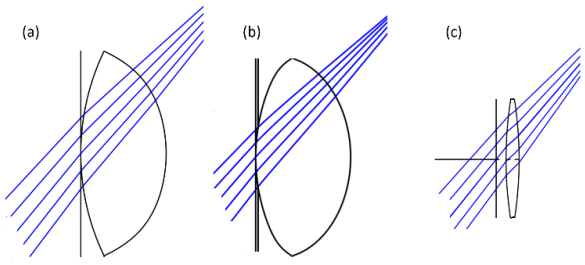

Fig 3. (a) Gullstrand-Emsley Lens profile. (b) Akram lens profile. (c) IOL lens profile.

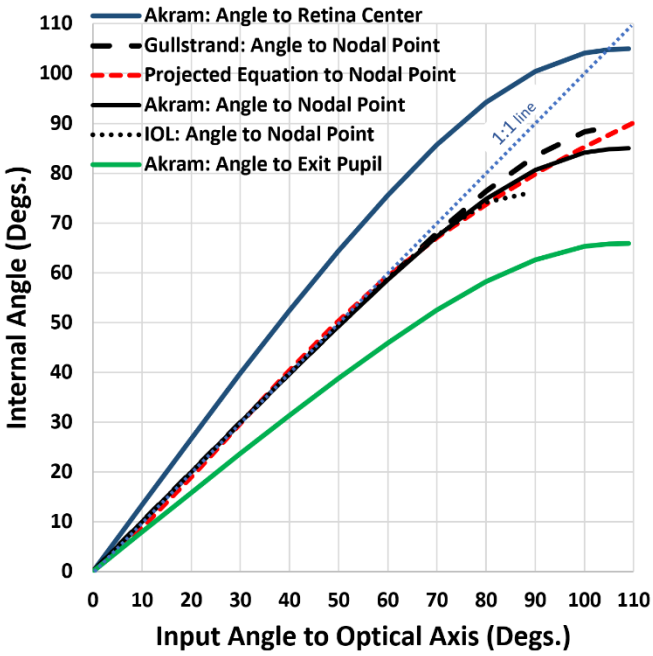

Fig 4. Internal angles from the 3 points of interest for the Akram model eye plotted against input angle to the optical axis. Angles for the other two model eyes to the nodal point are also plotted, along with the linear relationship, and a line that captures the general curvature of the relationships relative to the nodal point.

Light paths in the pseudophakic eye with a 2.5 mm internal pupil diameter were evaluated in more detail in Fig. 5 using Zemax footprint diagrams that indicates where rays are incident on a surface. A 2.5 mm internal stop diameter was used to enhance the vignetting effect, with clinical reports indicating that peripheral shadows are stronger for small pupils. The blue regions represent only rays that reach the retina, with the top plots showing the expected increasing ellipticity with angle for light entering the eye. This is similar to the elliptical appearance of the pupil at large angles[1], with the method used here capturing the rays of interest as they enter the eye. The second and 3rd rows show the proportions of the rays that are either focused by the IOL, or which miss the IOL. The 4th and 5th rows in Fig. 6 capture the proportions of the rays that after passing through the pupil are directed to the two image

locations. The pupil is always fully illuminated, but in the 4th row, as the input angle increases, the rays increasingly miss the IOL, and the effect of this can be seen in the 5th row.

The normalized energies directed to the two regions are plotted in Fig. 6 against radial input angle. The input light is directed to two separate regions of the retina, and light from a single input angle can appear to come from two separate object regions in the region where there is overlap. The maximum input angle is smaller than the value that might be expected for a phakic eye.

Estimates for the relative radial intensity on the retina for an evenly illuminated object field are given in Fig. 7. The "apparent" input angles that correspond to the retinal locations are estimated in the top plot using the angle at the nodal point (1:1), and in the bottom plot using the equation: input angle = $0.00011*x^3 - 0.0097*x^2 + 1.2$, where x is the angle at the nodal point. This is plotted as the "Projected Equation" in Fig.4, and it was estimated by eye to capture the main curving trend of the surrounding relationships, but without the flattening of those curves that causes a superposition of the data at very large angles. The plots both show that the main focused image, whose location on the retina can be related to actual input light angles, comes to an end. There is then a dark region, followed by the more peripheral retina being illuminated directly by light that misses the IOL. Both the scaling methods in Fig. 7 are relative rather than correct, but they characterize the questions surrounding the scaling of the peripheral retina with an IOL, where the illumination does not correspond to an input angle.

5. DISCUSSION

The modest non-linearity of the angular scaling of the retina at very large angles is known from the work of Drasdo et al[2] and Suheimat et al[3], who evaluated it from the perspective of scaling the physical details of the retina itself. At very large angles, the details of the eye model might be expected to become more important, and the more detailed Akram gradient index model eye here has a different curve to the simpler Gullstrand-Emsley eye model. For smaller angles, however, the relationship is highly linear up to 60 degrees for all the model eyes. This provides a simple concept for the eye, where the limits placed on visual angle by the nose, eyebrow and cheek at about that angle correspond to almost an entire retinal hemisphere for an average eye. In the temporal direction there is modest nonlinearity, but mostly at very large angles.

The IOL situation is quite different from the phakic eye at very large angles, despite there being relatively few clinical complaints. Even with the paraxial parameters in Fig 1, despite the IOL being much smaller than the crystalline lens, the nodal points are at a similar location, but the IOL surfaces are very different. At very large angles the light is not imaged by the IOL, yet depending on the iris location, light may also bypass the IOL and illuminate the retina directly. Scaling of this in various papers has used a linear relationship to estimate the input angles that corresponds to the increasing retinal locations [5,33]. This was an initial mechanism for establishing relative relationships, but the calculations here indicate that a modest non-linearity should be used instead in order to match the phakic eye more closely. However, the actual relationship depicted in Fig. 4 was found to be difficult to use because the curve flattened out, and a more plausible relationship was sketched instead for use in Fig. 7.

Fig 5. View from the rear of rays that reach the retina. The top plots cover an 8.2 mm diameter region that is always perpendicular to the incident light (with faint gridlines that have 0.82 mm spacing). The 2.5 mm diameter aperture at the iris in the lower plots is always fully illuminated.

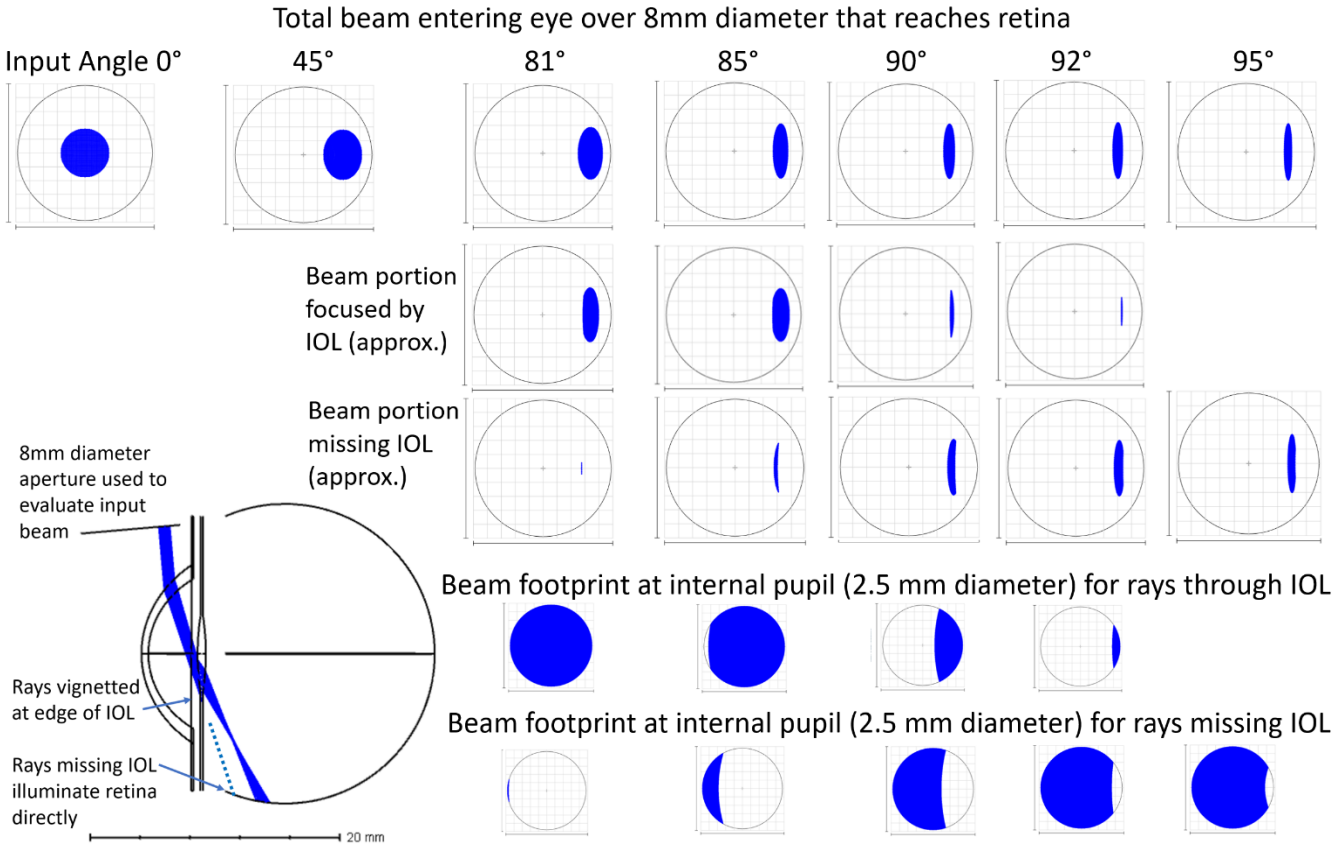

In practice, the calculations show that input light with an IOL is directed to two different retinal regions at very large angles, with no direct relationship between a single visual angle and a corresponding retinal region. It is not clear how the visual system deals with this, or if this scaling is involved with making peripheral shadows particularly "bothersome" for certain patients. There is a need for detailed investigation of the far peripheral visual region for both the phakic and the pseudophakic eye.

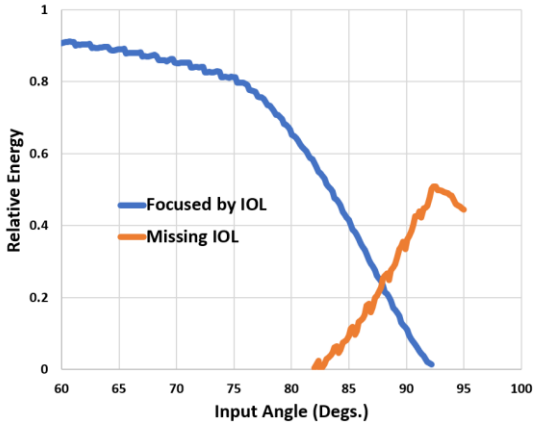

Fig 6. Energy reaching retina plotted against actual input angle, for the light focused by the IOL, and the light that misses the IOL. Internal pupil diameter 2.5 mm.

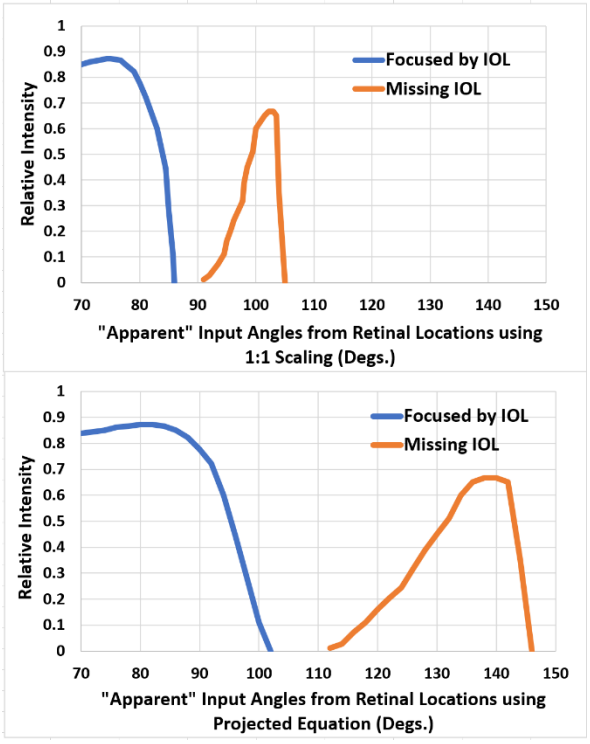

Fig 7. Estimated radial intensity on retina for eye with IOL and 2.5 mm pupil for even angular illumination. The curve was generated by integrating vertically across radial image points, and compensating for pupil ellipticity by dividing by 0.8 times the cosine of the angle. The top plot has 1:1 scaling from the retina to input angle. The bottom plot uses the equation described in the text.

Despite the uncertainty about the exact scaling of the modeling, and limited details about dark shadow complaints from patients, it is clear that with an IOL it is possible to get peripheral dark regions of the retina that are accompanied by illuminated regions more peripherally. The evaluation here considered a uniform input intensity, but it is likely that peripheral shadows are "bothersome" when there is strong object structure that modulates the peripheral light as the eye moves[6]. Several clinical solutions have been explored to resolve "negative dysphotopsia" [34], though they have had varying results. (a) "Reverse optic capture" surgery can be used, where the IOL is maneuvered to be positioned in front of the remaining lens capsule. This is thought to change the gap between the iris and the IOL[34]. (b) A second IOL can be inserted into the sulcus in front of the original IOL [25,28]. This is thought to change the optical properties in that region. (c) The original IOL can be changed for a different lens style, which can alter the optical characteristics [34]. (d) A larger IOL that is 7 mm rather than 6 mm in diameter can increase the size of the focused image and reduce the more peripheral light (though rays are actually so oblique at large angles that they become increasingly parallel to the lens)[35,36]. (e) The haptic region can be oriented to affect the peripheral rays.[37]. Alternative IOL designs have also been proposed, where light is deliberately redirected into the peripheral shadow region, but it is not clear if these have been pursued clinically [38–40].

Imaging aberrations due to either the cornea or the lens have not been addressed here in detail, and they would affect vision in the far periphery with either a phakic or a pseudophakic eye. Even for the cornea, however, which is widely measured by modern instrumentation, some of the most fundamental characterization is not performed. Light entering the eye at large angles has to pass through clear cornea, and although this is characterized by a white-to-white measurement from the front, this is not routinely related to the increasing corneal opacity that is visible from the side in an OCT image , where it often has a U or V shape[4,41,42]. Similarly, model eyes that have aspheric corneal surfaces may only be established for relatively modest visual angles, and one widely used model has a posterior corneal conic of -0.6 instead of about -0.25, which leads to the cornea having primarily a constant thickness, rather than having increasing thickness in the periphery[43]. Modeling the crystalline lens in the periphery is also a particular concern, and although an IOL can be characterized very well, the effects of residual capsular and other materials are difficult to measure and characterize. The modeling also used just a central wavelength of 0.546 microns and chromatic aberrations were not considered.

Overall, scaling the retina using the nodal point is a convenience rather than a requirement, and all 3 reference points described here are meaningful, with the exit pupil corresponding to the chief ray, and the center of the retinal sphere corresponding to the distance along the retinal surface. This topic is also relevant to the scaling of widefield retinal images, which use at least two different scaling methods [44,45], and where there is a lack of clarity about how the non-linearity at very large angles is addressed.

Funding. This paper is funded by Simpson Optics LLC with no external funding

Acknowledgments. Grateful thanks to anonymous reviewers.

Disclosures. MJS: Simpson Optics LLC (E).

Data availability. Data underlying the results presented in this paper are not publicly available at this time but may be obtained from the author upon reasonable request.

Conference Presentations: Presented in part at Visual and Physiological Optics, Cambridge UK, Aug. 2022.

References

1. Atchison DA, Smith G. *Optics of the Human Eye*. 2nd ed. CRC Press; 2023.
2. Drasdo N, Fowler CW. Non-linear projection of the retinal image in a wide-angle schematic eye. *Br J Ophthalmol*. 1974;58(8):709-714. doi:10.1136/bjo.58.8.709
3. Suheimat M, Zhu H, Lambert A, Atchison DA. Relationship between retinal distance and object field angles for finite schematic eyes. 2016;36(4):404-410. doi:10.1111/opo.12284
4. Simpson MJ. Mini-review: Far peripheral vision. *Vision Res*. 2017;140:96-104. doi:10.1016/j.visres.2017.08.001
5. Holladay JT, Simpson MJ. Negative dysphotopsia: Causes and rationale for prevention and treatment. *J Cataract Refract Surg*. 2017;43(2):263-275. doi:10.1016/j.jcrs.2016.11.049
6. Simpson MJ. Intraocular lens far peripheral vision: Image detail and negative dysphotopsia. *J Cataract Refract Surg*. 2020;46(3):451-458. doi:10.1097/j.jcrs.0000000000000103
7. Erie EA, Hodge DO, Mahr MA. Prevalence of pseudophakia: U.S. population – based study. *J Cataract Refract Surg*. 2022;48(6):717-722.
8. Holden BA, Fricke TR, Wilson DA, et al. Global Prevalence of Myopia and High Myopia and Temporal Trends from 2000 through 2050. *Ophthalmology*. 2016;123(5):1036-1042. doi:10.1016/j.ophtha.2016.01.006
9. Schaeffel F. Myopia - What is old and what is new? *Optom Vis Sci*. 2016;93(9):1022-1030. doi:10.1097/OPX.0000000000000914
10. Atchison DA, Li SM, Li H, et al. Relative peripheral hyperopia does not predict development and progression of myopia in children. *Investig Ophthalmol Vis Sci*. 2015;56(10):6162-6170. doi:10.1167/iovs.15-17200
11. Atchison DA, Rozema JJ. Technical notes on peripheral refraction, peripheral eye length and retinal shape determination. *Ophthalmic Physiol Opt*. 2023;(October 2022):1-11. doi:10.1111/opo.13097
12. Davison JA. Positive and negative dysphotopsia in patients with acrylic intraocular lenses. *J Cataract Refract Surg*. 2000;26(9):1346-1355.
13. Simpson MJ. Scaling the retinal image of the wide-angle eye using the nodal point. *Photonics*. 2021;8(7):1-9. doi:10.3390/photonics8070284
14. Simpson MJ. Nodal points and the eye. *Appl Opt*. 2022;61(10):2797. doi:10.1364/ao.455464
15. Simpson MJ. Focal length, EFL, and the eye. *Appl Opt*. 2023;62(7):1853-1857.
16. Beck C. The consideration of the equivalent planes of optical instruments. In: *The Proceedings of the Optical Convention*. Norgate & Williams, Covent Garden, London; 1905:9-18.
17. Bennett AG, Rabbetts RB. *Clinical Visual Optics*. 1st ed. Butterworths; 1984.
18. Smith WJ. *Modern Optical Engineering*. 2nd ed. McGraw-Hill; 1990.
19. Simpson MJ, Muzyka-Woźniak M. Iris characteristics affecting far peripheral vision and negative dysphotopsia. *J Cataract Refract Surg*. 2018;44(4):459-465. doi:10.1016/j.jcrs.2018.01.028
20. Hastings GD, Banks MS, Roorda A. Radial and tangential retinal magnifications as functions of visual field angle across spherical, oblate, and prolate retinal profiles. *Transl Vis Sci Technol*. 2022;11(9):1-17. doi:10.1167/tvst.12.1.8
21. Simpson MJ. Letter to the editor: radial and tangential retinal magnifications. *Transl Vis Sci Technol*. 2023;12(1):2022-2023. doi:10.1167/tvst.12.1.7
22. Hastings GD, Banks MS, Roorda A. Author Response: Radial and tangential retinal magnifications as functions of visual field angle across spherical, oblate, and prolate retinal profiles. *Transl Vis Sci Technol*. 2023;12(1):1-17. doi:10.1167/tvst.12.1.8
23. Atchison DA, Li SM, Li H, et al. Relative peripheral hyperopia does not predict development and progression of myopia in children. *Investig Ophthalmol Vis Sci*. 2015;56(10):6162-6170. doi:10.1167/iovs.15-17200
24. Makhotkina NY, Berendschot TTJM, Nuijts RMMA. Objective evaluation of negative dysphotopsia with Goldmann kinetic perimetry. *J Cataract Refract Surg*. 2016;42(11):1626-1633. doi:10.1016/j.jcrs.2016.09.016
25. Makhotkina NY, Dugrain V, Purchase D, Berendschot TTJM, Nuijts RMMA. Effect of supplementary implantation of a sulcus-fixated intraocular lens in patients with negative dysphotopsia. *J Cataract Refract Surg*. 2018;44(2):209-218. doi:10.1016/j.jcrs.2017.11.013
26. Simpson MJ. Simulated images of intraocular lens negative dysphotopsia and visual phenomena. *J Opt Soc Am A*. 2019;36(4):B44-B51. doi:10.1364/josaa.36.000b44
27. Masket S, Fram NR. Pseudophakic Dysphotopsia: A Review of Incidence, Etiology and Treatment of Positive and Negative Dysphotopsia. *Ophthalmology*. Published online 2020. doi:10.1016/j.ophtha.2020.08.009
28. Erie JC, Simpson MJ, Bandhauer MH. Effect of a sulcus-fixated piggyback intraocular lens on negative dysphotopsia: Ray-tracing analysis. *J Cataract Refract Surg*. 2018;45:443-450. doi:10.1016/j.jcrs.2018.10.041
29. Erie JC, Simpson MJ, Bandhauer MH. Influence of the intraocular lens optic–haptic junction on illumination of the peripheral retina and negative dysphotopsia. *J Cataract Refract Surg*. Published online 2019:1-5. doi:10.1016/j.jcrs.2019.04.019
30. Akram MNA, Baraas RC, Baskaran K. A wide-field emmetropic human eye model based on ocular wavefront measurements and geometry-independent gradient index lens. *J Opt Soc Am A*. 2018;35(11):1954-1967. doi:10.1364/JOSAA.35.001954
31. Bahrami M, Goncharov A V. Geometry-invariant

gradient refractive index lens: analytical ray tracing. *J Biomed Opt*. 2012;17(5):055001. doi:10.1117/1.JBO.17.5.055001
32. Fedtke C, Manns F, Ho A. The entrance pupil of the human eye: a three-dimensional model as a function of viewing angle. *Opt Express*. 2010;18(21):22364-22376. doi:10.1364/OE.18.022364
33. van Vught L, Luyten GPM, Beenakker JWM. Distinct differences in anterior chamber configuration and peripheral aberrations in negative dysphotopsia. *J Cataract Refract Surg*. 2020;46:1007-1015. doi:10.1097/j.jcrs.0000000000000206
34. Masket S, Fram NR, Cho A, Park I, Pham D. Surgical management of negative dysphotopsia. *J Cataract Refract Surg*. 2018;44(1):91-97. doi:10.1016/j.jcrs.2017.10.038
35. Erie JC, Simpson MJ, Mahr MA. Effect of a 7.0 mm intraocular lens optic on peripheral retinal illumination with implications for negative dysphotopsia. *J Cataract Refract Surg*. 2022;48(1):95-99. doi:10.1097/j.jcrs.0000000000000822
36. Bonsemeyer MK, Becker E, Liekfeld A. Dysphotopsia and functional quality of vision after implantation of an intraocular lens with a 7.0 mm optic and plate haptic design. *J Cataract Refract Surg*. 2022;48(1):75-82. doi:10.1097/j.jcrs.0000000000000735
37. Erie JC, Simpson MJ, Bandhauer MH. Influence of the intraocular lens optic–haptic junction on illumination of the peripheral retina and negative dysphotopsia. *J Cataract Refract Surg*. Published online 2019. doi:10.1016/j.jcrs.2019.04.019
38. Simpson M, Stanley D, Zhang X, Ellis K. IOL peripheral surface designs to reduce negative dysphotopsia. European Patent EP2152202B1. Published online 2010.
39. Erie JC, Simpson MJ, Bandhauer MH. A modified intraocular lens design to reduce negative dysphotopsia. *J Cataract Refract Surg*. 2019;45(7). doi:10.1016/j.jcrs.2019.01.019
40. Ho A. Intraocular lenses for reducing peripheral pseudophakic dysphotopsia. Patent Application WO 2021/181300 A1. Published online 2021.
41. Simpson MJ, Muzyka-Woźniak M. Iris characteristics affecting far peripheral vision and negative dysphotopsia. *J Cataract Refract Surg*. 2018;44(4):459-465. doi:10.1016/j.jcrs.2018.01.028
42. Muzyka-Woźniak M, Oleszko A, Stróżecki Ł, Woźniak S. The corneo-scleral junction assessed with optical coherence tomography. *PLoS One*. 2022;17(12 December):1-13. doi:10.1371/journal.pone.0278884
43. Liou HL, Brennan N a. Anatomically accurate, finite model eye for optical modeling. *J Opt Soc Am A Opt Image Sci Vis*. 1997;14(8):1684-1695. http://www.ncbi.nlm.nih.gov/pubmed/9248060
44. Toslak D, Son T, Erol MK, et al. Portable ultra-widefield fundus camera for multispectral imaging of the retina and choroid. *Biomed Opt Express*. 2020;11(11):6281. doi:10.1364/boe.406299
45. Yao X, Toslak D, Son T, Ma J. Understanding the relationship between visual-angle and eye-angle for reliable determination of the field-of-view in ultra-wide field fundus photography. *Biomed Opt Express*. 2021;12(10):6651. doi:10.1364/boe.433775